·论著·

高频双极脉冲不可逆电穿孔消融猪肝组织的安全性和有效性研究

袁晶[1]　董守龙[2]　陈玉潇[1]　李廷源[1]　何闯[1]　李良山[1]　陈林[3]　姚陈果[2]　黄学全[1]
[1]陆军军医大学第一附属医院血管外科,重庆　400038;[2]重庆大学电气工程学院　400030;
[3]陆军军医大学第一附属医院放射科,重庆　400038
通信作者:黄学全,Email:hxuequan@163.com

【摘要】　目的　探讨高频双极脉冲不可逆电穿孔(IRE)消融猪肝组织的安全性和有效性。**方法**　采用实验研究方法。采用陆军军医大学实验中心巴马小型猪 18 只,雌雄不限,月龄为(6.8±0.8)个月,月龄范围为 5.5~8.0 个月。18 只巴马小型猪按随机数字表法分为实验组(15 只)和对照组(3 只),实验组巴马小型猪行高频双极脉冲 IRE 消融,于消融结束后即刻、消融后第 3、7、14、28 天各取 3 只行增强 CT 检查后处死,取肝组织行组织病理学检查;对照组巴马小型猪行单极脉冲 IRE 消融,于消融后第 3 天行增强 CT 检查后处死,取肝组织行组织病理学检查。检测指标:(1)两组巴马小型猪肌肉收缩强度比较。(2)实验组巴马小型猪 IRE 消融后 CT 增强检查影像学表现。(3)实验组巴马小型猪 IRE 消融后组织病理学表现。(4)两组巴马小型猪 IRE 消融后消融区肝组织细胞凋亡指数比较。正态分布的计量资料以 *Mean*±*SD* 表示,组间比较采用独立样本 *t* 检验。**结果**　(1)两组巴马小型猪肌肉收缩强度比较:两组巴马小型猪均成功完成 IRE 消融。实验组巴马小型猪术中肌肉收缩强度为(9.8±0.4)m/s^2,对照组为(48.6±0.5)m/s^2,两组比较,差异有统计学意义($t=-163.50$,$P<0.05$)。(2)实验组巴马小型猪 IRE 消融前后 CT 增强检查影像学表现:IRE 消融结束后即刻、消融后第 7 天,实验组巴马小型猪 CT 增强检查见消融区呈低密度影,边界清晰,消融区内及其毗邻大血管未见明显异常,消融后均未出现严重并发症。随消融后时间延长,实验组消融区与正常肝组织边界逐渐模糊,消融区逐渐被正常肝组织替代,消融后第 28 天增强 CT 检查可见消融区明显缩小甚至消失。实验组巴马小型猪 IRE 消融后消融区最长径:消融后即刻为(1.81±0.17)cm、消融后第 3 天为(1.75±0.19)cm、消融后第 7 天为(1.32±0.22)cm、消融后第 14 天为(0.65±0.14)cm、消融后第 28 天为(0.28±0.10)cm。(3)实验组巴马小型猪 IRE 消融后组织病理学表现:消融后即刻,实验组巴马小型猪苏木素伊红染色组织病理学检查示消融区细胞肿胀,排列紊乱,部分针道周围可见出血;消融后第 3 天 HE 染色组织病理学检查示消融区内胆管与血管形态完整,可见大量深染细胞核、部分溶解或裂开的细胞核和凋亡小体,消融区周围可见大量炎性细胞浸润;消融后第 3 天血管性血友病因子染色组织病理学检查示完整的血管内皮细胞;消融后第 3 天原位末端标记法染色检查示消融区内大量核深染的凋亡细胞显著多于消融区外;消融后第 3 天 Von Kossa 染色检查示部分黑褐色钙盐沉积;消融后第 7、14、28 天均可见大量新生的肝细胞从消融区周边向中心生长,且随时间延长呈逐渐增多趋势;消融后第 14、28 天均可见平滑肌细胞增生;消融后第 28 天消融区基本被新生细胞替代。(4)两组巴马小型猪 IRE 消融后消融区肝组织细胞凋亡指数比较:实验组和对照组巴马小型猪 IRE 消融后第 3 天消融区肝组织细胞凋亡指数分别为 76.67%±0.04%和 64.03%±0.05%,两组比较,差异有统计学意义($t=4.79$,$P<0.05$)。**结论**　高频双极脉冲 IRE 消融猪肝组织安全、有效,且比单极脉冲 IRE 消融更加彻底。

【关键词】　消融技术;　肝组织;　高频双极脉冲;　不可逆电穿孔;　巴马小型猪
基金项目:国家自然科学基金青年科学基金项目(51807016);重庆市社会民生科技创新专项(cstc2015shmszx120033)
DOI:10.3760/cma.j.issn.1673-9752.2019.10.014

Analysis of safety and efficacy of irreversible electroporation hepatic ablation with high-frequency bipolar pulse in swine

Yuan Jing[1], Dong Shoulong[2], Chen Yuxiao[1], Li Tingyuan[1], He Chuang[1], Li Liangshan[1], Chen Lin[3], Yao Chenguo[2], Huang Xuequan[1]
[1]Department of Vascular Surgery, the First Hospital Affiliated to Army Medical University, Chongqing 400038, China; [2]Electrical Engineering Academy of Chongqing University, Chongqing 400030, China; [3]Department of

Radiology, the First Hospital Affiliated to Army Medical University, Chongqing 400038, China
Corresponding author: Huang Xuequan, Email: hxuequan@163.com

【**Abstract**】 **Objective** To investigate the safety and efficacy of irreversible electroporation (IRE) hepatic ablation with high-frequency bipolar pulse in swine. **Methods** The experimental study was conducted. A total of 18 swines of either gender, aged (6.8+0.8) months with a range of 5.5−8.0 months, were collected from Animal Laboratory Center of Army Medical University. were randomly divided into 15 in experimental group and 3 in control group. The swines in experimental group underwent IRE hepatic ablation with high-frequency bipolar pulse, and 3 swines were chose randomly and underwent enhanced CT examination immediately after ablation, and at 3, 7, 14, and 28 days after ablation. The liver tissues were taken for histopathological examination. The swines in the control group underwent IRE hepatic ablation with high-frequency monopolar burst, and was performed enhanced CT examination at 3 days after ablation. Liver tissues were taken for histopathological examination. Observation indicators: (1) comparison of muscle contraction of siwnes between two groups; (2) imaging performance on enhanced CT after IRE ablation in the experimental group; (3) hepatic histopathological findings after IRE ablation in the experimental group; (4) comparison of apoptotic index in the ablation zone between two groups. The measurement data with normal distribution were expressed as *Mean*±*SD*, and comparison between groups was performed by the independent sample *t* test. **Results** (1) Comparison of muscle contraction between two groups: swines in both groups underwent ablation successfully. The degree of muscle contraction was (9.8±0.4) m/s^2 and (48.6±0.5) m/s^2 in the experimental group and in the control group, respectively, showing statistically significant difference between the two groups ($t=-163.50$, $P<0.05$). (2) Imaging performance on enhanced CT after IRE ablation in the experimental group: the enhanced CT examination of swines immediately after IRE ablation showed a low-density shadow and clear boundary in the ablation zone. There was no obvious abnormality in the ablation zone and its adjacent large vessels. No serious complications occurred after the ablation. The boundary between the ablation zone and the normal liver tissue of the experimental group gradually became blurred over time, and the ablation zone was gradually replaced by normal liver tissue. The ablation zone at the 28 days after ablation was significantly reduced or even disappeared on imaging of enhanced CT examination. The maximum diameter of the ablation zone was (1.81±0.17) cm immediately after ablation, (1.75±0.19) cm at the 3 days after ablation, (1.32±0.22) cm at the 7 days after ablation, (0.65±0.14) cm at the 14 days after ablation, (0.28±0.10) cm at the 28 days after ablation, respectively. (3) Hepatic histopathological findings after IRE ablation in the experimental group: the HE staining of ablated tissue immediately after ablation showed that the cells in the ablation zone were swollen, arranged disorderly, and bleeding was observed around some of the needles. The bile ducts and blood vessels were intact in the ablation zone, and a large number of deeply stained nuclei were seen at 3 days after ablation, some of the nucleus and apoptotic bodies were partially dissolved or cleaved. A large number of inflammatory cell were infiltrated around the ablation zone. Intact vascular and biliary endothelial cells were observed by von Willebrand factor staining, a larger number of apoptotic cells with deeply stained nuclei in the ablation zone were observed by terminal-deoxynucleoitidyl transferase mediated nick end labeling staining, and partial deposited dark brown calcium salt was seen by Von Kossa staining. More newborn hepatocytes were observed growing from the periphery of the ablation zone to the center at the 7, 14, 28 days after ablation. Smooth muscle cell proliferation was observed at 14 and 28 days after ablation. The ablation zone was replaced by new cells on 28 days after ablation. (4) Comparison of apoptotic index in the ablation zone between two groups: the apoptotic index of the ablation zone was significantly higher in the experimental group than in the control group on the 3 days after operation (76.67%±0.04% *vs.* 64.03%±0.05%, $t=4.79$, $P<0.05$). **Conclusion** IRE hepatic ablation of swine using high-frequency bipolar pulse is safe and reliable, and it has more apoptotic cells than IRE ablation with high-frequency monopolar burst.

【**Key words**】 Ablation; Swine; Hepatic issues; High-frequency bipolar pulse; Irreversible electroporation

Fund programs: National Natural Science Foundation of China for Youth (51807016); Social Life and Technological Innovation Project of Chongqing (cstc2015shmszx 120033)

DOI: 10.3760/cma.j.issn.1673-9752.2019.10.014

临床实践中以外科手术切除、放射治疗等常规方法处理毗邻血管或其他重要组织器官的肿瘤时，存在一定局限与禁忌。近年来，不可逆电穿孔(irreversible electroporation，IRE)技术的应用显著提高了此类肿瘤的治疗效果。IRE 为非热消融技术，其原理是利用 μs 和 ns 高强度单极脉冲作用于细胞膜的磷脂双分子层，打破肿瘤细胞内外生理平衡，使细胞膜发生不可恢复的“孔洞”，导致细胞凋亡；可在有效消融肿瘤的同时，避免周围血管、神经、胆管、尿道等正常组织结构损伤[1-5]。IRE 技术现已应用于肝

脏、胰腺、肾脏和前列腺等部位实体肿瘤的临床治疗[6-23]。然而,消融不彻底和术中可引起肌肉收缩两大难题限制了 IRE 技术推广[24]。针对单极脉冲消融肿瘤的局限性,姚陈果[25]自主研发出高频双极脉冲 IRE 设备。本研究采用高频双极脉冲 IRE 消融巴马小型猪的肝组织,探讨其安全性和有效性。

1　材料与方法

采用实验研究方法。

1.1　材料

巴马小型猪 18 只,雌雄不限,月龄为(6.8±0.8)个月,月龄范围为 5.5~8.0 个月;体质量为(16±3)kg,体质量范围为 10~20 kg,由陆军军医大学动物实验中心提供,动物实验许可证号:SCXK[(渝)20170002]。新型复合脉冲治疗仪样机及其配套电极针由重庆大学自主研发,国家食品药品监督管理局上海医疗器械质量监督检验中心注册:国医检(设)字 ZC2017 第 177 号;该设备能够产生单、双极脉冲,脉冲电压可达±3 kV,脉冲宽度在 100 ns~100 μs 范围内连续可调,脉冲上升、下降时间均为 30 ns,脉冲串内重复频率最高可达 2 MHz,脉冲串重复频率为 0.1~10.0 Hz。采用联影 uCT510 型 16 排螺旋 CT 扫描仪及 Analog Device ADXL335 高精度三轴加速度传感器作为引导及监测设备。

1.2　方法

1.2.1　分组:18 只巴马小型猪按随机数字表法分为实验组(15 只)和对照组(3 只),分别对实验组和对照组巴马小型猪行高频双极脉冲 IRE 消融和单极脉冲 IRE 消融。

1.2.2　消融处理:消融前,对两组巴马小型猪均禁饲食、饮水>12 h;并以留置针穿刺耳缘静脉建立通道,采用3%戊巴比妥钠溶液按 1 mL/kg 行静脉注射麻醉和维持麻醉。将巴马小型猪左侧卧位放置于 CT 检查床上,对其右侧腹部术区备皮,体表放置自制定位栅;行 CT 平扫检查后确定进针点和穿刺路径。每只巴马小型猪的肝脏任选 3 个部位(如胆囊旁、肝静脉旁、门静脉旁等)行 CT 检查引导下 IRE 消融,每个部位平行穿刺入 2 根 19 G 消融电极探针,针间距 1 cm,探针针尖裸露部分长 1 cm,每个部位距离其中一根针距离≤5 mm。分别对实验组和对照组巴马小型猪进行 IRE 消融,实验组采用高频双极脉冲,脉冲参数设置:100 个重复频率 1 Hz 的脉冲串,脉冲串脉宽度 100 μs,每个脉冲串内包含 20 个正负交替的子脉冲,子脉冲宽度 5 μs,各子脉冲间隔 10 μs,脉冲电压 1 500 V;对照组采用单极脉冲方案:100 个重复频率 1 Hz、脉冲宽度 100 μs 的单极脉冲,脉冲电压 1 500 V。脉冲施加方案示意图见图 1。在巴马小型猪腹直肌下部放置高精度三轴加速度传感器,记录脉冲处理过程中的肌肉收缩情况。

1.2.3　消融后处理:消融结束后巴马小型猪即刻行 CT 增强检查,观察消融情况及气胸、出血、血管狭窄、胆汁漏等并发症发生情况。如发现并发症,必要时对症处理;如无并发症或仅为无需处理的轻微并发症,则在穿刺点消毒、覆盖敷贴并待巴马小型猪麻醉苏醒后,将其送回动物房喂养。

1.2.4　标本采集:实验组 15 只巴马小型猪分别于消融结束后即刻、消融后第 3、7、14、28 天各取 3 只行增强 CT 检查后大剂量注射 3%戊巴比妥钠溶液处死;将消融区肝组织切块后,放置于 4%多聚甲醛溶液中脱水、固定,行组织病理学观察。对照组于消融后第 3 天行增强 CT 检查后处死、取材,行组织病理学观察。

1.3　检测指标

(1)两组巴马小型猪肌肉收缩强度比较。(2)实验组巴马小型猪 IRE 消融后 CT 增强检查影像学表现:消融区 CT 增强检查影像学特征变化、消融区最长径。(3)实验组巴马小型猪 IRE 消融后组织病理学表现:将固定的实验组巴马小型猪消融区肝

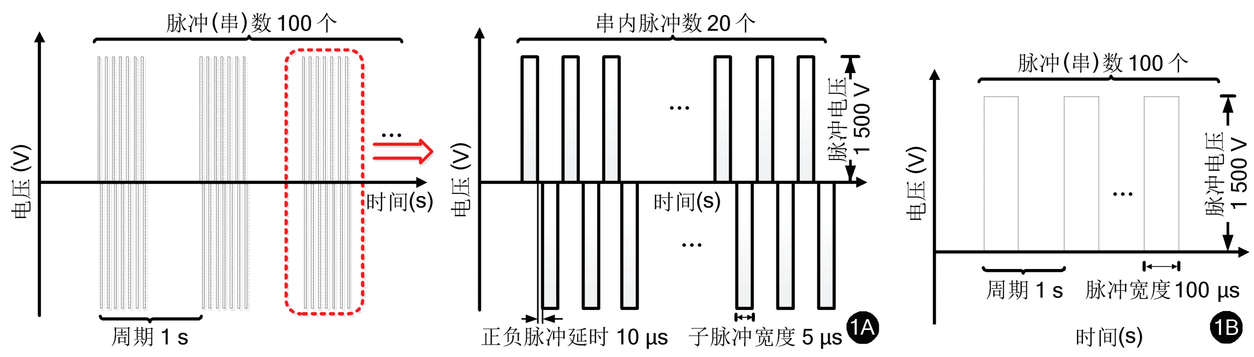

图 1　巴马小型猪不可逆电穿孔消融脉冲施加方案示意图　1A:高频双极脉冲示意图;1B:单极脉冲示意图

组织分别行 HE、血管性血友病因子(von Willebrand factor, vWF)、原位末端标记法(terminal-deoxynucleoitidyl transferase mediated nick end labeling, TUNEL)、Von Kossa 染色检测。(4)两组巴马小型猪 IRE 消融后消融区肝组织细胞凋亡指数比较:两组巴马小型猪消融区肝组织进行 TUNEL 细胞凋亡检测,计算两组消融后第 3 天消融区肝组织细胞凋亡指数。

1.4　统计学分析

应用 SPSS 20.0 统计软件进行分析。正态分布的计量资料以 *Mean*±*SD* 表示,组间比较采用独立样本 t 检验。$P<0.05$ 为差异有统计学意义。

2　结果

2.1　两组巴马小型猪肌肉收缩强度比较

两组巴马小型猪均成功完成 IRE 消融。实验组巴马小型猪术中肌肉收缩强度为(9.8±0.4) m/s^2,对照组为(48.6±0.5) m/s^2,两组比较,差异有统计学意义($t=-163.50$, $P<0.05$),见图 2。

2.2　实验组巴马小型猪 IRE 消融后 CT 增强检查影像学表现

将 IRE 消融前 CT 检查图像作为对照,IRE 消融后即刻、消融后第 7 天,实验组巴马小型猪 CT 增强检查均可见消融区呈低密度影,边界清晰,消融区内及其毗邻大血管未见明显异常,无血管狭窄及对比剂外漏等现象。见图 3。实验组巴马小型猪处死前增强 CT 检查均未见明显血管狭窄、门静脉血栓、胆瘘、胆囊坏死等严重并发症。随消融后时间延长,实验组消融区与正常肝组织边界逐渐模糊,消融区逐渐被正常肝组织替代,消融后第 28 天增强 CT 检查可见消融区明显缩小甚至消失(图 3F)。实验组巴马小型猪 IRE 消融后消融区最长径:消融后即刻为(1.81±0.17) cm、消融后第 3 天为(1.75±0.19) cm、消融后第 7 天为(1.32±0.22) cm、消融后第 14 天为(0.65±0.14) cm、消融后第 28 天为(0.28±0.10) cm。

2.3　实验组巴马小型猪 IRE 消融后组织病理学表现

IRE 消融后即刻,实验组巴马小型猪 HE 染色组织病理学检查示消融区细胞肿胀,排列紊乱,部分针道周围可见出血。见图 4A。消融后第 3 天 HE 染色组织病理学检查消融区内胆管与血管形态完整,可见大量深染细胞核、部分溶解或裂开的细胞核和凋亡小体,消融区周围可见大量炎性细胞浸润。见图 4B。消融后第 3 天 vWF 染色组织病理学检查示消融区血管、胆管内膜完整,内皮细胞无破坏。见图 4C。消融后第 3 天 TUNEL 染色检查示消融区内大量核深染的凋亡细胞显著多于消融区外。见图 4D。消融后第 3 天 Von Kossa 染色检查示部分黑褐色钙盐沉积。见图 4E。消融后第 7、14、28 天均可见大量新生肝细胞从消融区周边向中心生长,且随时间延长呈逐渐增多趋势;消融后第 14、28 天均可见平滑肌细胞增生;消融后第 28 天消融区基本被新生细胞替代。见图 4F。

2.4　两组巴马小型猪 IRE 消融后消融区肝组织细胞凋亡指数比较

实验组和对照组巴马小型猪 IRE 消融后第 3 天消融区肝组织细胞凋亡指数分别为 76.67%±0.04% 和 64.03%±0.05%,两组比较,差异有统计学意义($t=4.79$, $P<0.05$)。

3　讨论

与常见的单极脉冲 IRE 设备比较,新型复合脉冲治疗仪的优势在于输出脉冲波形为高频双极性脉冲串,子脉冲电压幅值正反交替,负脉冲引起动作电位反向,减缓了由正脉冲引起的肌细胞动作电位上升,使得细胞膜电位升高不能达到阈值、不触发动作电位出现肌肉强烈收缩,从而达到均匀电场分布和抑制局部区域肌肉收缩的目的[26-29]。

本研究采用高频双极脉冲 IRE 成功消融巴马小型猪在体肝组织,CT 增强检查示消融结束后消融

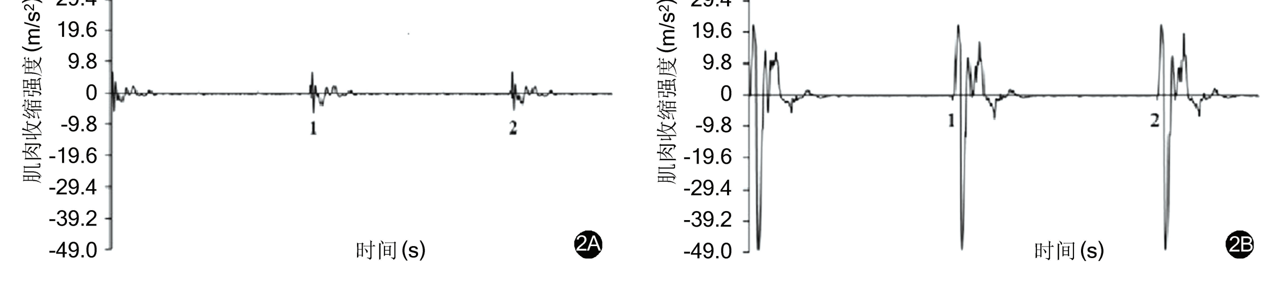

图 2　实验组和对照组巴马小型猪不可逆电穿孔消融术中肌肉收缩情况　2A:实验组采用高频双极脉冲;2B:对照组采用单极脉冲

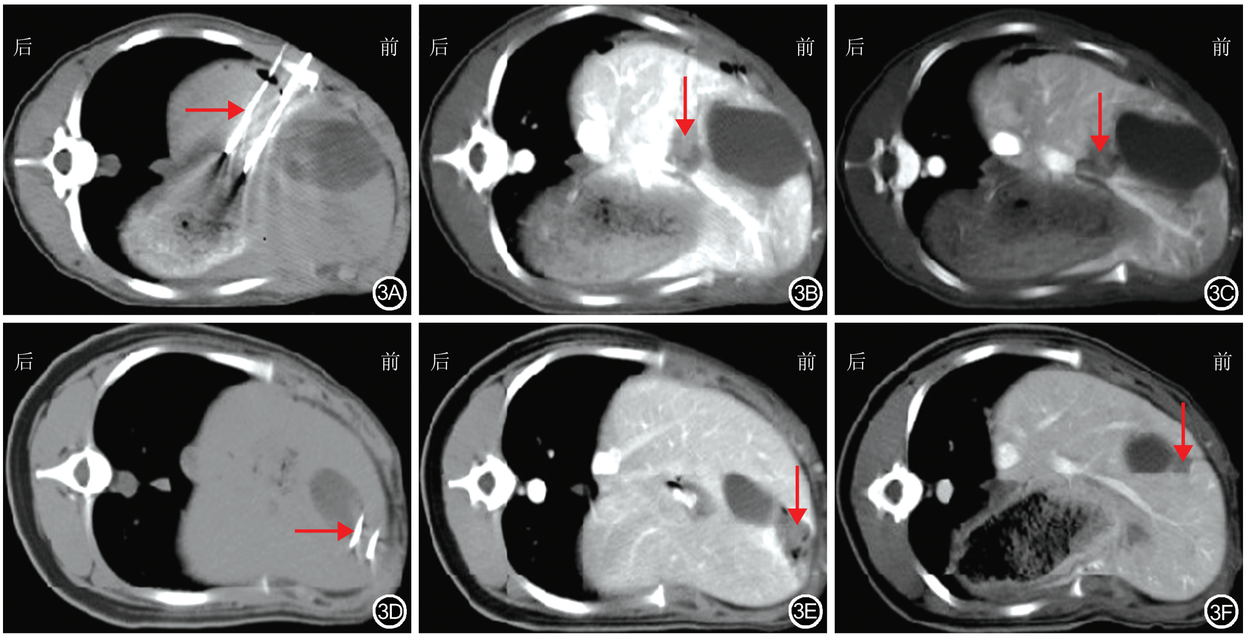

注:巴马小型猪呈左侧卧位;实验组采用高频双极脉冲

图 3　实验组巴马小型猪高频双极脉冲不可逆电穿孔消融前后增强 CT 检查结果　3A:消融前 CT 检查引导下将 2 根 19 G 消融电极探针(→)平行插入实验猪门静脉旁肝组织中作为对照;3B:消融后即刻增强 CT 检查示消融区(↓)边界清晰,其内有正常强化的血管影,血管远端未见狭窄;3C:消融后第 7 天增强 CT 检查示消融区(↓)均呈低密度影,门静脉远端走行正常,消融区较前稍缩小;3D:消融前 CT 检查引导下将 2 根 19 G 消融电极探针(→)平行插入实验猪胆囊旁肝组织作为对照;3E:消融后即刻增强 CT 检查示胆囊壁完整未见破坏,消融后即刻消融区(↓)毗邻胆囊壁呈低密度影;3F:消融后第 28 天增强 CT 检查示消融区完全消失,胆囊旁肝组织内可见纤维条索影(↓)

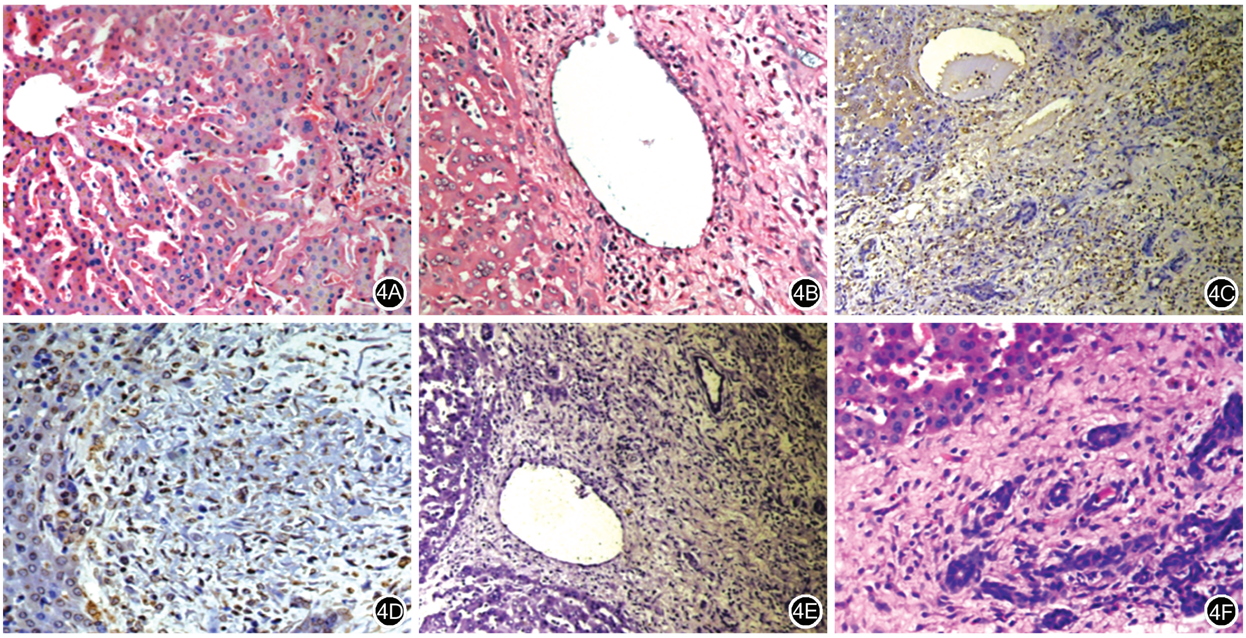

注:实验组采用高频双极脉冲

图 4　实验组巴马小型猪高频双极脉冲不可逆电穿孔消融后肝组织病理学检查结果　4A:消融后即刻,消融区肝窦扩张充血,肝细胞水肿　HE 染色　中倍放大;4B:消融后第 3 天,消融区大量核碎片,可见细胞凋亡细胞,消融区周围可见大量炎性细胞浸润 HE 染色　中倍放大;4C:消融后第 3 天,消融区内血管、胆管结构完整,未见明显破坏　血管性血友病因子染色　低倍放大;4D:消融后第 3 天消融区内可见大量深染的凋亡细胞　原位末端标记法染色　中倍放大;4E:消融后第 3 天,消融区内可见大量黑褐色钙盐沉积　Von Kossa 染色　中倍放大;4F:消融后第 28 天,肝组织内见条索纤维、肝细胞和胆管等大量增生,消融区基本消失　HE 染色　中倍放大

区毗邻动脉、静脉、胆管等无明显损伤；在消融胆囊旁肝组织时，即使电极针紧贴胆囊壁，消融后可见边界清晰的消融区与胆囊壁毗邻，亦未见胆囊壁破坏；消融门静脉分支区域时消融区内静脉正常显影，无远端血管狭窄等。其主要原因为 IRE 消融时通过施加脉冲在探针针尖周围形成局部高电场，场内细胞的膜电位发生改变，脉冲击穿细胞膜形成不可逆性穿孔、破坏细胞内环境导致细胞死亡，而不会破坏纤维组织等非细胞结构。因此，IRE 消融与以射频、微波为代表的温度消融比较，在血管、胆管、尿道、神经等部位肿瘤消融时拥有优势。2017 年 Siddiqui 等[30]采用高频双极脉冲 IRE 消融小型猪肝脏，其研究结果亦证实消融血管和胆囊旁组织安全、可靠。由于 IRE 消融时产生细胞凋亡，消融区内细胞会再生，因此，随着消融后时间延长，其消融区将会被正常肝细胞逐渐取代，增强 CT 检查示消融区逐渐减小，最终与正常肝脏强化一致。

本研究结果显示：消融结束后即刻消融区肝细胞明显水肿，可见细胞凋亡；7 d 后可见消融区逐渐被新生肝细胞和纤维结缔组织逐渐取代，CT 增强检查表现与 HE 染色组织病理学结果相符。张欣等[31]采用 IRE 消融小型猪肝脏的研究结果显示：消融消融后第 3 天凋亡细胞最多。本研究结果显示：实验组巴马小型猪肝组织消融后第 3 天消融区肝组织细胞凋亡指数显著高于对照组。这表明 IRE 消融时可产生更多凋亡细胞，提示高频双极脉冲较单极脉冲 IRE 消融更为有效。2017 年重庆大学姚成果团队采用流式细胞术检测传统 IRE 脉冲与复合脉冲作用下细胞的死亡途径，其研究结果显示：复合脉冲与传统 IRE 脉冲比较，能引起更高比例的细胞凋亡[32]。高频双极性脉冲比单极脉冲消融产生更多凋亡细胞的主要原因为高频双极性脉冲不仅能够破坏细胞膜结构，同时也能够破坏细胞核膜，而单极脉冲不能破坏细胞核膜[33]。

为避免局部肌肉收缩震颤对 IRE 治疗的影响，有时需使用肌松剂。然而，在使用肌松剂后，消融则需在全身静脉麻醉和监护下进行。2018 年 Mafeld 等[12]的研究结果显示：与单极脉冲 IRE 消融比较，高频双极脉冲 IRE 消融更有利于降低肌肉收缩强度。2016 年 Siddiqui 等[30]的研究结果显示：采用高频双极脉冲 IRE 消融猪肝组织，其肌肉收缩强度较低，认为无需使用肌松剂。本研究消融时未使用肌松剂，实验组消融中肌肉收缩强度低于对照组，这提示采用高频双极脉冲 IRE 消融有利于减少甚至避免术中肌松剂的使用，使更多消融可在局部麻醉下完成，从而扩大 IRE 的适用范围。2017 年 Yao 等[29]通过使用复合脉冲消融兔子肝脏探讨不同参数与消融面积和肌肉收缩强度之间的关系，其研究结果显示：复合脉冲脉宽宽度越小，其肌肉收缩程度越小，消融面积也会减小。

本研究存在以下不足：(1) 虽然 IRE 属于非热消融，但有实验研究结果表明 IRE 电极探针附近仍旧会出现热损伤[34-35]。本研究未对消融过程中的热损伤进行分析。(2) 由于本研究未使用肌松剂，消融时的局部肌肉收缩可能影响消融范围。因为肌肉收缩会导致探针相对位置发生位移，导致电场分布发生变化，影响消融区。未来有望采用单针进行不可逆电穿孔消融，这将会在消融过程中保证消融效果和消融区更加可预测，不需要保证多针平行，并且极大降低因多针穿刺导致的组织损伤相关并发症的发生率[36-37]。(3) 与单极脉冲 IRE 比较，高频双极脉冲 IRE 消融猪肝的肝组织凋亡指数更高，但其对肿瘤消融的有效性仍待进一步通过荷瘤动物证实。

综上，高频双极脉冲 IRE 消融猪肝组织安全、有效，且比单极脉冲 IRE 消融更加彻底。

利益冲突　所有作者均声明不存在利益冲突

参 考 文 献

[1] Luo X, Qin Z, Tao H, et al. The Safety of irreversible electroporation on nerves adjacent to treated tumors[J]. World Neurosurg, 2017, 108(12): 642-649. DOI: 10.1016/j.wneu.2017.09.049.

[2] Vogel JA, Van VE, Agnass P, et al. Time-dependent impact of irreversible electroporation on pancreas, liver, blood vessels and nerves: a systematic review of experimental studies[J]. PloS One, 2016, 11(11): e0166987. DOI: 10.1371/journal.pone.0166987.

[3] Tschon M, Salamanna F, Ronchetti M, et al. Feasibility of electroporation in bone and in the surrounding clinically relevant structures: a preclinical investigation[J]. Technol Cancer Res Treat, 2016, 15(6): 737-748. DOI: 10.1177/1533034615604454.

[4] Wendler JJ, Pech M, Porsch M, et al. Urinary tract effects after multifocal nonthermal irreversible electroporation of the kidney: acute and chronic monitoring by magnetic resonance imaging, intravenous urography and urinary cytology[J]. Cardiovasc Intervent Radiol, 2012, 35(4): 921-926. DOI: 10.1007/s00270-011-0257-0.

[5] Tam AL, Figueira TA, Gagea M, et al. Irreversible electroporation in the epidural space of the porcine spine: effects on adjacent structures[J]. Radiology, 2016, 281(3): 763-771. DOI: 10.1148/radiol.2016152688.

[6] Ruarus AH, Lgph V, Puijk RS, et al. Irreversible electroporation in hepatopancreaticobiliary tumours[J]. Can Assoc Radiol J, 2018, 69(1): 38-50. DOI: 10.1016/j.carj.2017.10.005.

[7] 秦子淋，曾健滢，牛立志．不可逆电穿孔消融治疗肝恶性肿瘤现状[J]．介入放射学杂志，2017，26(3)：285-289. DOI：10.3969/j.issn.1008-794X.2017.03.023.

[8] Lyu T, Wang X, Su Z, et al. Irreversible electroporation in primary and metastatic hepatic malignancies: a review[J]. Medicine, 2017, 96(17): e6386. DOI: 10.1097/MD.0000000000006386.

[9] Giorgio A, Amendola F, Calvanese A, et al. Ultrasound-guided percutaneous irreversible electroporation of hepatic and abdominal tumors not eligible for surgery or thermal ablation: a western report on safety and efficacy[J]. J Ultrasound, 2019, 22(1): 53-58. DOI:10.1007/s40477-019-00372-7.

[10] Stillström D, Beermann M, Engstrand J, et al. Initial experience with irreversible electroporation of liver tumours[J]. Eur J Radiol Open, 2019, 6: 62-67. DOI:10.1016/j.ejro.2019.01.004.

[11] Kalra N, Gupta P, Gorsi U, et al. Irreversible Electroporation for Unresectable Hepatocellular Carcinoma: Initial Experience[J]. Cardiovasc Intervent Radiol, 2019, 42(4): 584-590. DOI: 10.1007/s00270-019-02164-2.

[12] Mafeld S, Wong JJ, Kibriya N, et al. Percutaneous irreversible electroporation (IRE) of hepatic malignancy: a bi-institutional analysis of safety and outcomes[J]. Cardiovasc Intervent Radiol, 2019, 42(4): 577-583. DOI:10.1007/s00270-018-2120-z.

[13] Distelmaier M, Barabasch A, Heil P, et al. Midterm safety and efficacy of irreversible electroporation of malignant liver tumors located close to major portal or hepatic veins[J]. Radiology, 2017, 285(3): 1023-1031. DOI:10.1148/radiol.2017161561.

[14] Ansari D1, Kristoffersson S1, Andersson R, et al. The role of irreversible electroporation (IRE) for locally advanced pancreatic cancer: a systematic review of safety and efficacy[J]. Scand J Gastroenterol, 2017, 52(11): 1165-1171. DOI: 10.1080/00365521.2017.1346705.

[15] Huang KW, Yang PC, Pua U, et al. The efficacy of combination of induction chemotherapy and irreversible electroporation ablation for patients with locally advanced pancreatic adenocarcinoma[J]. J Surg Oncol, 2018, 118(1): 31-36. DOI:10.1002/jso.25110.

[16] Field W, Rostas JW, Martin RCG. Quality of life assessment for patients undergoing irreversible electroporation (IRE) for treatment of locally advanced pancreatic cancer (LAPC)[J]. Am J Surg, 2019[Epub ahead of print]. pii: S0002-9610(18)31405-3. DOI:10.1016/j.amjsurg.2019.03.020.

[17] Tasu JP, Vesselle G, Herpe G, et al. Irreversible electroporation for locally advanced pancreatic cancer: where do we stand in 2017? [J]. Pancreas, 2017, 46(3): 283-287. DOI: 10.1097/MPA.0000000000000793.

[18] Wendler JJ, Pech M, Fischbach F, et al. Initial assessment of the efficacy of irreversible electroporation in the focal treatment of localized renal cell carcinoma with delayed-interval kidney tumor resection (irreversible electroporation of kidney tumors before partial nephrectomy [IRENE] trial-an ablate-and-resect pilot study) [J]. Urology, 2018, 114(4): 224-232. DOI: 10.1016/j.urology.2017.12.016.

[19] Sorokin I, Lay AH, Reddy NK, et al. Pain after percutaneous irreversible electroporation of renal tumors is not dependent on tumor location[J]. J Endourol, 2017, 31(8): 751-755. DOI: 10.1089/end.2017.0201.

[20] Distelmaier M, Barabasch A, Heil P, et al. Midterm safety and efficacy of irreversible electroporation of malignant liver tumors located close to major portal or hepatic veins[J]. Radiology, 2017, 285(3): 1023-1031. DOI:10.1148/radiol.2017161561.

[21] Scheltema MJ, van den Bos W, de Bruin DM, et al. Focal vs extended ablation in localized prostate cancer with irreversible electroporation; a multi-center randomized controlled trial[J]. BMC cancer, 2016, 16(1): 299. DOI:10.1186/s12885-016-2332-z.

[22] Campelo S, Valerio M, Ahmed HU, et al. An evaluation of irreversible electroporation thresholds in human prostate cancer and potential correlations to physiological measurements[J]. APL Bioeng, 2017, 1(1): 016101. DOI:10.1063/1.5005828.

[23] van den Bos W, de Bruin DM, Muller BG, et al. The safety and efficacy of irreversible electroporation for the ablation of prostate cancer: a multicentre prospective human in vivo pilot study protocol[J]. BMJ Open, 2014, 10(4): e006382. DOI: 10.1136/bmjopen-2014-006382.

[24] Philips P, Li Y, Li S, et al. Efficacy of irreversible electroporation in human pancreatic adenocarcinoma: advanced murine model[J]. Mol Ther Methods Clin Dev, 2015, 2: 15001. DOI: 10.1038/mtm.2015.1.

[25] 姚陈果.新型复合脉冲不可逆电穿孔治疗肿瘤关键技术及临床应用研究进展[J].高电压技术,2018,44(1):248-263. DOI:10.13336/j.1003-6520.hve.20171227031.

[26] Sano MB, Fesmire CC, DeWitt MR. Burst and continuous high frequency irreversible electroporation protocols evaluated in a 3D tumor model[J]. Phys Med Biol, 2018, 13(63): 135022. DOI:10.1088/1361-6560/aacb62.

[27] Mercadal B, Arena CB, Davalos RV, et al. Avoiding nerve stimulation in irreversible electroporation: a numerical modeling study [J]. Phys Med Biol, 2017, 62(20): 8060-8079. DOI: 10.1088/1361-6560/aa8c53.

[28] Sano MB, Fan RE, Cheng K, et al. Reduction of muscle contractions during irreversible electroporation therapy using high-frequency bursts of alternating polarity pulses: a laboratory investigation in an exvivo swine model[J]. J Vasc Interv Radiol, 2018, 29(6): 893-898. DOI:10.1016/j.jvir.2017.12.019.

[29] Yao C, Dong S, Zhao Y, et al. Bipolar microsecond pulses and insulated needle electrodes for reducing muscle contractions during irreversible electroporation[J]. IEEE Trans Biomed Eng, 2017, 64(12): 2924-2937. DOI:10.1109/TBME.2017.2690624.

[30] Siddiqui IA, Kirks RC, Latouche EL, et al. High-frequency irreversible electroporation: safety and efficacy of next-generation irreversible electroporation adjacent to critical hepatic structures[J]. Surg Innov, 2017, 24(3): 276-283. DOI: 10.1177/1553350617692202.

[31] 张欣,肖越勇,杜鹏,等.经皮纳米刀消融小型猪肝组织的安全性及有效性[J].中国介入影像与治疗学,2015,12(5):259-262. DOI:10.13929/j.1672-8475.2015.05.002.

[32] Yao CG, Zhao YJ, Mi Y, et al. Comparative study of the biological responses to conventional pulse and high-frequency monopolar pulse bursts[J]. IEEE Transactions on Plasma Science, 2017, 45(10): 2629-2638. DOI:10.1109/TPS.2017.2703091.

[33] Ivey JW, Latouche EL, Sano MB, et al. Targeted cellular ablation based on the morphology of malignant cells[J]. Sci Rep, 2015, 5: 17157. DOI:10.1038/srep17157.

[34] Dunki-Jacobs EM, Philips P, Martin RC 2nd. Evaluation of thermal injury to liver, pancreas and kidney during irreversible electroporation in an in vivo experimental model[J]. Br J Surg, 2014, 101(9): 1113-1121. DOI:10.1002/bjs.9536.

[35] Faroja M, Ahmed M, Appelbaum L, et al. Irreversible electroporation ablation: is all the damage nonthermal? [J]. Radiology, 2013, 266(2): 462-470. DOI:10.1148/radiol.12120609.

[36] O'Brien TJ, Passeri M, Lorenzo MF, et al. Experimental high-frequency irreversible electroporation using a single-needle delivery approach for nonthermal pancreatic ablation in vivo[J]. J Vasc Interv Radiol, 2019, 30(6): 854-862. e7. DOI: 10.1016/j.jvir.2019.01.032.

[37] Sano MB, DeWitt MR, Teeter SD. Optimization of a single insertion electrode array for the creation of clinically relevant ablations using high-frequency irreversible electroporation[J]. Comput Biol Med, 2018, 95(4): 107-117. DOI: 10.1016/j.compbiomed.2018.02.009.

（收稿日期：2019-07-09）

本文引用格式

袁晶,董守龙,陈玉潇,等.高频双极脉冲不可逆电穿孔消融猪肝组织的安全性和有效性研究[J].中华消化外科杂志,2019,18(10):979-985. DOI:10.3760/cma.j.issn.1673-9752.2019.10.014.

Yuan Jing, Dong Shoulong, Chen Yuxiao, et al. Analysis of safety and efficacy of irreversible electroporation hepatic ablation with high-frequency bipolar pulse in swine[J]. Chin J Dig Surg, 2019, 18(10): 979-985. DOI:10.3760/cma.j.issn.1673-9752.2019.10.014.